catalysts

MDPI

Article

(*S*)-Pramipexole and Its Enantiomer, Dexpramipexole: A New Chemoenzymatic Synthesis and Crystallographic Investigation of Key Enantiomeric Intermediates

Samuele Ciceri [1,*], Patrizia Ferraboschi [1], Paride Grisenti [2], Shahrzad Reza Elahi [1], Carlo Castellano [3], Matteo Mori [4] and Fiorella Meneghetti [4,*]

[1] Department of Medical Biotechnology and Translational Medicine, University of Milan, Via C. Saldini 50, 20133 Milano, Italy; patrizia.ferraboschi@unimi.it (P.F.); shahrzad.rezaelahi@gmail.com (S.R.E.)
[2] Chemical-Pharmaceutical Consulting and IP Management, Viale G. da Cermenate 58, 20141 Milano, Italy; grisenti.paride60@gmail.com
[3] Department of Chemistry, University of Milan, Via C. Golgi 19, 20133 Milano, Italy; carlo.castellano@unimi.it
[4] Department of Pharmaceutical Sciences, University of Milan, Via L. Mangiagalli 25, 20133 Milano, Italy; matteo.mori@unimi.it
* Correspondence: samuele.ciceri@guest.unimi.it (S.C.); fiorella.meneghetti@unimi.it; (F.M.); Tel.: +39-0250-316-052 (S.C.); +39-0250-319-306 (F.M.)

Received: 13 July 2020; Accepted: 13 August 2020; Published: 16 August 2020

Abstract: A new chemoenzymatic method has been developed for the synthesis of (*S*)- and (*R*)-*N*-(6-hydroxy-4,5,6,7-tetrahydrobenzo[d]thiazol-2-yl) acetamide, two key synthons for the preparation of (*S*)-pramipexole, an anti-Parkinson drug, and its enantiomer dexpramipexole, which is currently under investigation for the treatment of eosinophil-associated disorders. These two building blocks have been obtained in good yields and high enantiomeric excess (30% and >98% ee for the *R*-enantiomer, and 31% and >99% ee for the *S*- one) through a careful optimization of the reaction conditions, starting from the corresponding racemic mixture and using two consecutive irreversible transesterifications, catalyzed by *Candida antarctica* lipase type A. Single crystal X-ray analysis has been carried out to unambiguously define the stereochemistry of the two enantiomers, and to explore in depth their three-dimensional features.

Keywords: chiral synthons; pramipexole; dexpramipexole; Parkinson's disease; hypereosinophilic syndromes; biocatalysis; asymmetric synthesis; *Candida antarctica* Lipase A; irreversible transesterification; crystal structures

1. Introduction

Pramipexole is a dopamine agonist approved for the treatment of Parkinson's disease and for restless legs syndrome; it is marketed as dihydrochloride salt under the brand name Mirapex [1–3].

Pramipexole or 2-amino-6-propylamino-4,5,6,7-tetrahydrobenzothiazole **1**, has a stereogenic center on C6 (Figure 1), and only the isomer (*S*)-**1** exhibits anti-Parkinson properties. The isomer (*R*)-**1**, also known as dexpramipexole, was studied some years ago for the treatment of ALS (amyotrophic lateral sclerosis) [4–6]; however, despite the promising results in early clinical studies, its development was discontinued in 2013, due to a lack of efficacy observed in a Phase 3 study [7,8]. More recently, a reduction in the absolute eosinophil count (AEC), coincidentally detected during the ALS-related clinical development, suggested a possible application of dexpramipexole for the treatment of eosinophil-associated disorders [9,10].

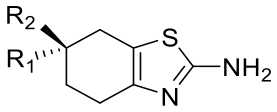

(*S*)-**1**. R_1= $NHCH_2CH_2CH_3$, R_2= H
(*R*)-**1**. R_1= H, R_2= $NHCH_2CH_2CH_3$

Figure 1. Structures of pramipexole (*S*)-**1** and dexpramipexole (*R*)-**1**.

The optical purity of this compound is a crucial parameter in the synthetic process, due to the different activities of the two enantiomers.

Usually, the *rac*-**1** or its precursor, the amine *rac*-**2** (Figure 2), are resolved by fractional crystallization of a diastereomeric salt [11,12] or by preparative chiral high-performance liquid chromatography (HPLC) [13,14].

Taking into account the promising results of our previous experiments [15], in which a *Saccharomyces cerevisiae*-catalyzed reduction of ketone **3** (Figure 2) afforded the optically pure (*R*)-**4** (Figure 2), and considering the few chemoenzymatic approaches [16,17] available for the synthesis of pramipexole, we studied the resolution of the alcohol *rac*-**4** by means of an enzymatic transformation. The enantiopure alcohol (*R*)-**4** proved to be a useful synthon for the synthesis of (*S*)-**1** dihydrochloride monohydrate, the commercial form of this active ingredient, in five steps and 21% overall yield [15].

The alcohols (*R*)-**4** and (*S*)-**4** (Figure 2) were here studied by means of single-crystal X-ray diffraction, which represents the best approach to unambiguously characterize chiral compounds, as confirmed by our successful application of this technique to the structural analysis of several optically active molecules [18,19].

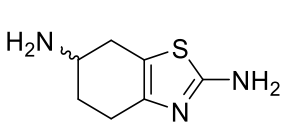

rac-**2**

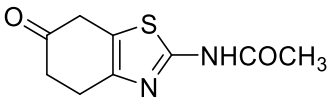

3

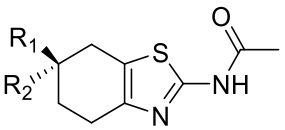

(*R*)-**4**. R_1= OH, R_2= H
(*S*)-**4**. R_1= H, R_2= OH

Figure 2. Structures of amine *rac*-**2**, ketone **3**, alcohol (*R*)-**4** and its isomer (*S*)-**4**.

2. Discussion and Results

2.1. Lipase-Catalyzed Preparation of Alcohols (R)-4 and (S)-4

Two enzyme-catalyzed preparations of the suitable synthon of (*S*)-**1** are reported in the literature. In a 2006 patent [17], the enzyme-catalyzed resolution of diamine *rac*-**2** was described: among the screened enzymes, only *Candida antarctica* lipase A (CAL-A), under acylation conditions, and some lipases from *Pseudomonas* sp. afforded promising results (100% ee determined by HPLC analysis of the non-isolated diamine **2** or the corresponding amide **5**) (Scheme 1A). The 2-acetylamino-4,5,6,7-tetrahydrobenzothiazole-6-carboxylic acid **7** was resolved in 2007 by Riva et al. through a CAL-B-catalyzed hydrolysis of the corresponding ester, affording the optically pure ester (*S*)-**6** (by HPLC analysis) at 55% conversion [16] (Scheme 1, B). The (*S*)-acid can be converted into (*S*)-**1** through a rearrangement, described in a 2005 patent [20].

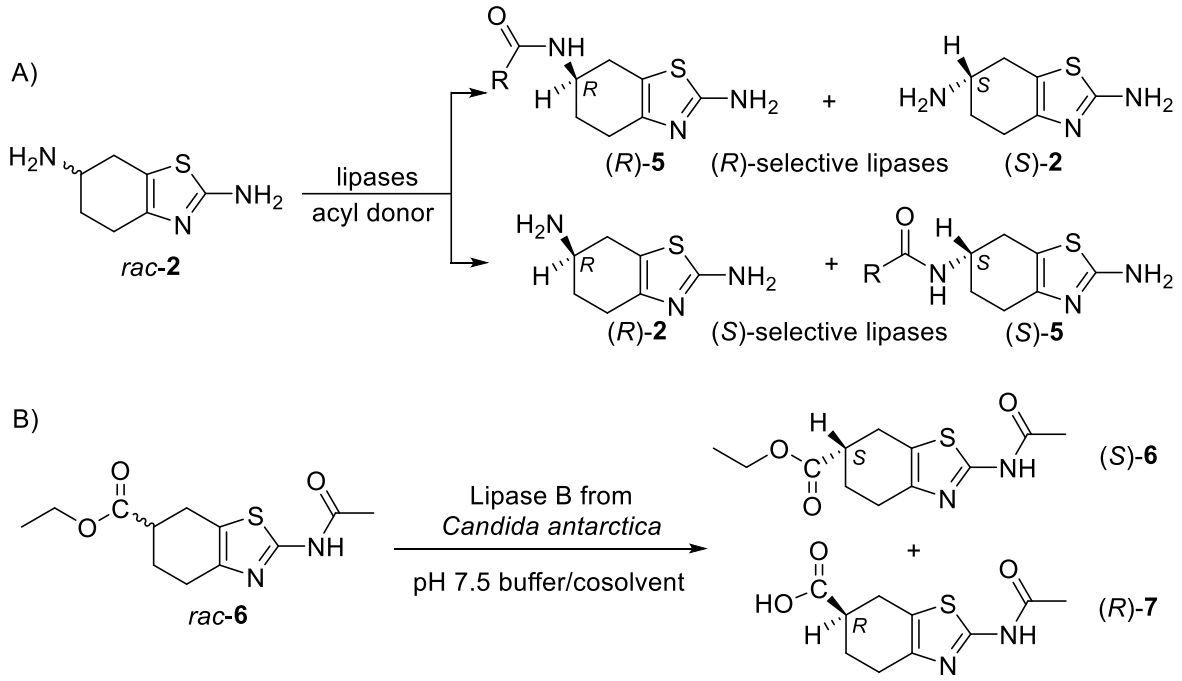

Scheme 1. (**A**) Enzyme-catalyzed resolution of *rac*-**2** [17]; (**B**) enzyme-catalyzed resolution of *rac*-**6** [16].

In 2014, we prepared the alcohol (*R*)-**4** in 79% yield and >98% ee from the 6-ketone **3** by means of a bio-reduction catalyzed by *Saccharomyces cerevisiae*, common baker's yeast [15]. This synthon was used as a suitable precursor of (*S*)-**1**; the same (*R*)-**4** was also used as starting material for the synthesis of (*R*)-**1**, after an inversion of configuration carried out through a Mitsunobu reaction, unfortunately characterized by a tedious purification process and low yield (27%) (Scheme 2).

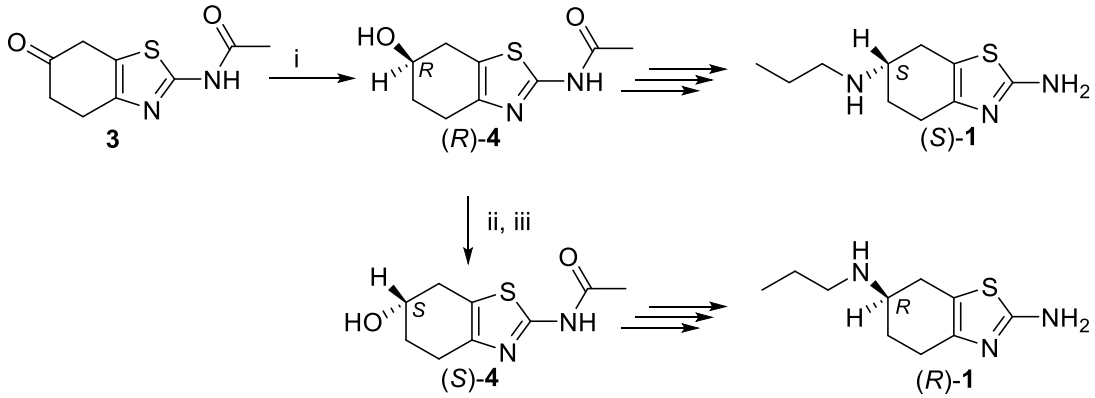

Scheme 2. i) Baker's yeast, pH 7 buffer, heptane, 79%, >98% ee; **ii**) PhCOOH, diethyl azodicarboxylate (DEAD), Ph_3P, DMF; **iii**) 1% NaOH, methanol [15].

Once the suitable enzyme has been identified, the well-known advantage [21–23] offered by an enzymatic kinetic resolution of a racemic alcohol is the obtainment of both enantiomers as optically pure substances, while the reduction of a ketone catalyzed by a microorganism, including *Saccharomyces cerevisiae* [15], affords only one enantiomer. The 6-hydroxy derivative of the 2-aminotetrahydrobenzothiazole, compound **8** [15], could be a substrate of a hydrolytic enzyme, but preliminary attempts of resolution by means of common lipases resulted in a concurrent acylation of the 6-hydroxyl and 2-amino groups (Scheme 3).

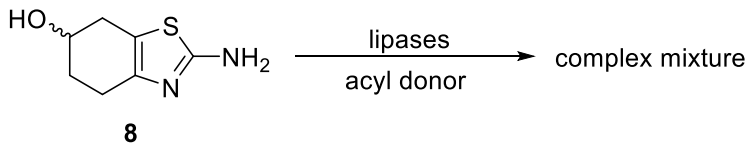

Scheme 3. First attempt of enzyme-catalyzed resolution of compound **8**.

Hence, a screening was carried out choosing as substrate the acetate *rac*-**9**, which is the acetyl ester of the alcohol *rac*-**4**, obtained by the sodium borohydride-mediated reduction of ketone **3**. The most common commercially available lipases and a cross-linked preparation of the protease subtilisin (Alcalase® CLEA) were used under hydrolytic conditions (phosphate buffer pH 7). Only the lipase from porcine pancreas (PPL) proved to be inactive, whereas the other tested enzymes were able to remove the acetyl group, albeit with an unsatisfactory ee (Table 1 and Scheme 4).

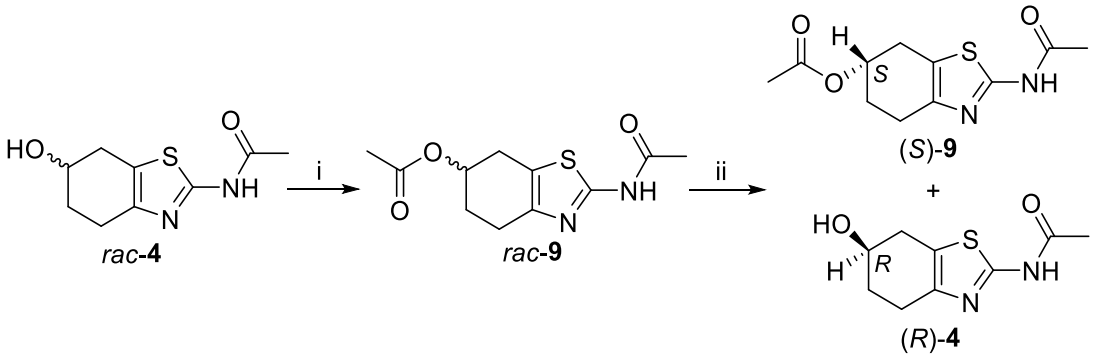

Scheme 4. Enzyme-catalyzed hydrolysis of acetate *rac*-**9**. **i**) Ac_2O, py; **ii**) hydrolytic enzyme, pH 7 buffer.

Table 1. Enzyme-catalyzed hydrolysis of acetate *rac*-**9**.

Entry	Enzyme	Time (h)	Conversion[a] (%)	ee (%)[a]		Config.[c] of formed **4**
				Acetate **9**	Alcohol **4**	
a	PPL	168	0	-	-	-
b	PFL	312	22	-	16	*R*
c	CAL-A	30	46	-	39	*R*
d	CAL-B	120	54	31[b]	-	*R*
e	CCL	120	64	38[b]	-	*S*
f	Alcalase CLEA	96	30	-	37	*R*

[a]determined by chiral high-performance liquid chromatography (HPLC) analysis. [b]determined after hydrolysis of acetate. [c]by comparison with the data reported in Ref. [15].

The alcohol (*R*)-**4** for the synthesis of (*S*)-**1** was obtained with all the enzymes, with the exception of the lipase from *Candida cylindracea* (CCL), which led to the opposite enantiomer (*S*)-**4**. The low ee, also observed under alcoholysis conditions, prompted us to study the enzyme-catalyzed transesterification of alcohol *rac*-**4**. The use of trifluoroethyl butyrate as acyl donor and the lipase from *Pseudomonas fluorescens* (PFL) or CAL-A as enzymes, which emulated the reaction conditions reported in the 2006 patent for the resolution of *rac*-**2** [17], did not provide encouraging results: PFL did not work, and CAL-A afforded a low conversion (7%) to the corresponding butyrate, showing a 43% ee.

Furthermore, the irreversible transesterification [24,25], using vinyl acetate as acyl donor and tetrahydrofuran (THF) as solvent, afforded an unsatisfactory ee (Table 2 and Scheme 5), with the best

results being observed in the case of PFL- or CAL-A-catalyzed transformations (68% ee for (*R*)-**9**, 20–23% conversion).

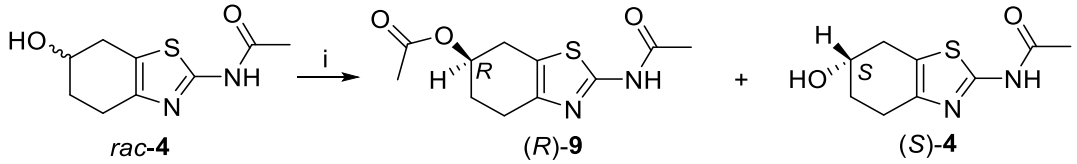

rac-**4** (*R*)-**9** (*S*)-**4**

Scheme 5. Enzyme-catalyzed irreversible transesterification of alcohol *rac*-**4**. (i) hydrolytic enzyme, vinyl acetate, tetrahydrofuran (THF).

Table 2. Enzyme-catalyzed irreversible transesterification of alcohol *rac*-**4** in THF.

Entry	Enzyme	Time (h)	Conversion[a] (%)	ee[a]		Config. of unreacted 4
				Acetate 9	Alcohol 4	
a	Alcalase CLEA	168	0	-	-	-
b	*Rhizopus oryzae* lipase	168	0	-	-	-
c	PPL	168	<5	-	-	*S*
d	*Aspergillus niger* lipase	168	14	20[b]		*S*
e	CAL-B	7	60		28	*S*
f	CCL	168	20	41[b]		*R*
g	PFL	73	20	68[b]		*S*
h	CAL-A	168	23	68[b]		*S*

[a]determined by chiral HPLC analysis. [b] determined after hydrolysis of acetate.

These rather promising results encouraged us to perform a solvent screening: besides THF, *rac*-**4** showed an appreciable solubility in acetone, methyl isobutyl ketone (MIBK), dimethyl sulfoxide, and dimethylformamide. Among them, the choice was addressed to the two less hydrophilic options, namely MIBK and acetone. Moreover, toluene was selected to study the outcome of the enzyme-catalyzed transesterification when carried out in a hydrophobic solvent, characterized by a lesser ability to strip off the essential water from the surface of the enzymes [26], but unable to solubilize the substrate *rac*-**4**. In this case, lipases afforded good reaction rates but a low enantioselectivity. Conversely, when employing MIBK as solvent, moderate reaction yield and enantioselectivity were observed. In acetone, PFL and CCL were found to be inactive, most likely due to the higher hydrophilicity of acetone compared to MIBK; however, CAL-A showed a good enantioselectivity, albeit at the expense of the reaction rate. To establish if the results obtained with MIBK and acetone were satisfactory for practical purposes, the E (enantiomeric ratio) values were calculated according to Rakels et al. [27]. An enzymatic resolution displays a preparative significance only if its E is >10 [28–31]. While the E observed in the case of the CAL-A-catalyzed resolution in MIBK was 12, which is enough to obtain enantiomers with ee values >98% after a second enzymatic resolution [29], the E of the CAL-A-catalyzed transformation in acetone was 28, thus indicating the possibility to obtain more satisfactory results in terms of optical purity and yields (Table 3).

Table 3. Enzyme-catalyzed irreversible transesterification of *rac*-**4** in toluene, methyl isobutyl ketone (MIBK) and acetone.

Entry	Enzyme	Solvent	Time (h)	Conversion[a] (%)	ee[a] (%)		E[c]	Config. of unreacted 4
					Acetate 9	Alcohol 4		
a	PFL	Toluene	72	35	15[b]	9	1	*S*
b	CAL-A	Toluene	16	62	6[b]	10	1	*S*
c	CCL	Toluene	4	45	26[b]	20	2	*R*
d	PFL	MIBK	168	33	72[b]	26	8	*S*
e	CAL-A	MIBK	23	64	61[b]	91	12	*S*
f	CCL	MIBK	120	51	53[b]	45	5	*R*
g	PFL	Acetone	168	-	-	-	-	-
h	CAL-A	Acetone	168	34	89[b]	50	28	*S*
i	CCL	Acetone	168	-	-	-	-	-

[a]determined by chiral HPLC analysis. [b]determined after hydrolysis of acetate. [c]$E = \ln[(1-ee_s)/(1+ee_s/ee_p)]/\ln[(1+ee_s)/(1+ee_s/ee_p)]$.

Following the findings by Herbst, Peper, and Niemeyer [26], we also studied the possibility to mitigate the tendency of acetone to remove the essential water molecules from the enzyme by adding water (1 μL of distilled water/mL of acetone) or mixing it with *n*-hexane, with the aim of reaching a good reaction rate together with a similar enantioselectivity to that obtained in pure acetone. The performed tests and the obtained results are summarized in Table 4.

Table 4. CAL-A-catalyzed irreversible transesterification of *rac*-**4** in acetone with the addition of water or *n*-hexane.

Entry	Solvent	Time (h)	Conversion[a] (%)	ee[a] (%)		E[c]
				Acetate 9	Alcohol 4	
a	Acetone + 0.1% H_2O	336	32	90[b]	37	27
b	Acetone/*n*-hexane 1:1	32	69	47[b]	>99	14
c	Acetone/*n*-hexane 2:1	95	50	79[b]	75	19
d	Acetone/*n*-hexane 4:1	168	45	83[b]	68	22

[a]determined by chiral HPLC analysis. [b]determined after hydrolysis of acetate. [c]$E = \ln[(1-ee_s)/(1+ee_s/ee_p)]/\ln[(1+ee_s)/(1+ee_s/ee_p)]$.

The results reported in Table 4 show that the addition of *n*-hexane had a great impact on both the enantioselectivity and the reaction rate. The higher the amount of *n*-hexane in the reaction medium, the higher the reaction rate was, but at the expense of the enantioselectivity. In particular, comparing pure acetone to the acetone/*n*-hexane 1:1 mixture, we observed an increase in the reaction rate (from 168 h for a 34% conversion to 32 h for a 69% conversion) and a decrease in the enantioselectivity (the E values changed from 28 to 14). These findings are in agreement with those reported by Herbst et al. [26]: the conversion rate of a kinetic resolution catalyzed by a lipase decreases with a stepwise increase of the solvent hydrophilicity (in our case with the increase of the acetone content); at the same time, the higher the hydrophilicity of the reaction medium, the higher the enantioselectivity. This behavior can be explained by the ability of the hydrophilic medium to extract the essential water of the enzymes, thus lowering their activity. At the same time, an enzyme with less essential water has a highly rigid structure, which allows it to better discriminate between the two enantiomers, leading to an increased enantioselectivity. In this context, it is interesting to note the linear dependence between the E-value and the amount of *n*-hexane in acetone, observed in the selected range (Figure 3). Moreover, the drop in activity of CAL-A with the addition of 0.1% water to the solvent (336 h for a 32% conversion) was previously explained by Herbst et al. [26]: under certain conditions, the addition of water can lead to enzyme agglomeration up to denaturation.

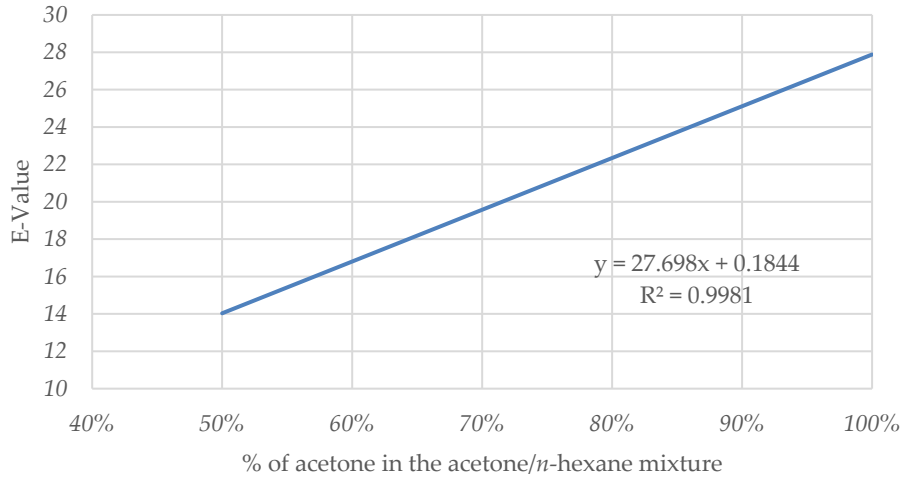

Figure 3. E-value versus acetone/*n*-hexane ratio of CAL-A-catalyzed irreversible transesterification of *rac*-**4**.

According to the results summarized in Table 4 and Figure 3, the catalytic system employing the mixture acetone/*n*-hexane 4:1 as solvent can be considered a good compromise between enantioselectivity and reactivity, with the aim to synthesize enantiopure (*R*)- and (*S*)-**4**.

The first CAL-A-catalyzed transesterification was carried out starting from the racemic alcohol *rac*-**4**. 91% ee (*S*)-**4** and 75% ee (*R*)-**9** were obtained (E-value of 22) at 58% conversion (about 300 h) after chromatographic purification. The 91% ee alcohol (*S*)-**4** was used as substrate in a second CAL-A-catalyzed transesterification in order to obtain enantiopure (*S*)-**4** (>99% ee at 12% conversion). The 75% ee acetate (*R*)-**9** was hydrolyzed to yield enantioenriched (*R*)-**4**, used as substrate in a second CAL-A-catalyzed transesterification. This second enzymatic resolution was stopped at 78% conversion. (*R*)-**9** was isolated by means of chromatographic purification, affording >98% ee (*R*)-**4** after hydrolysis. The isolated enantiopure alcohols (*S*)-**4** and (*R*)-**4** show the necessary configurations for the preparation of dexpramipexole (*R*)-**1** and pramipexole (*S*)-**1**, according to the previously optimized method [15] (Scheme 6).

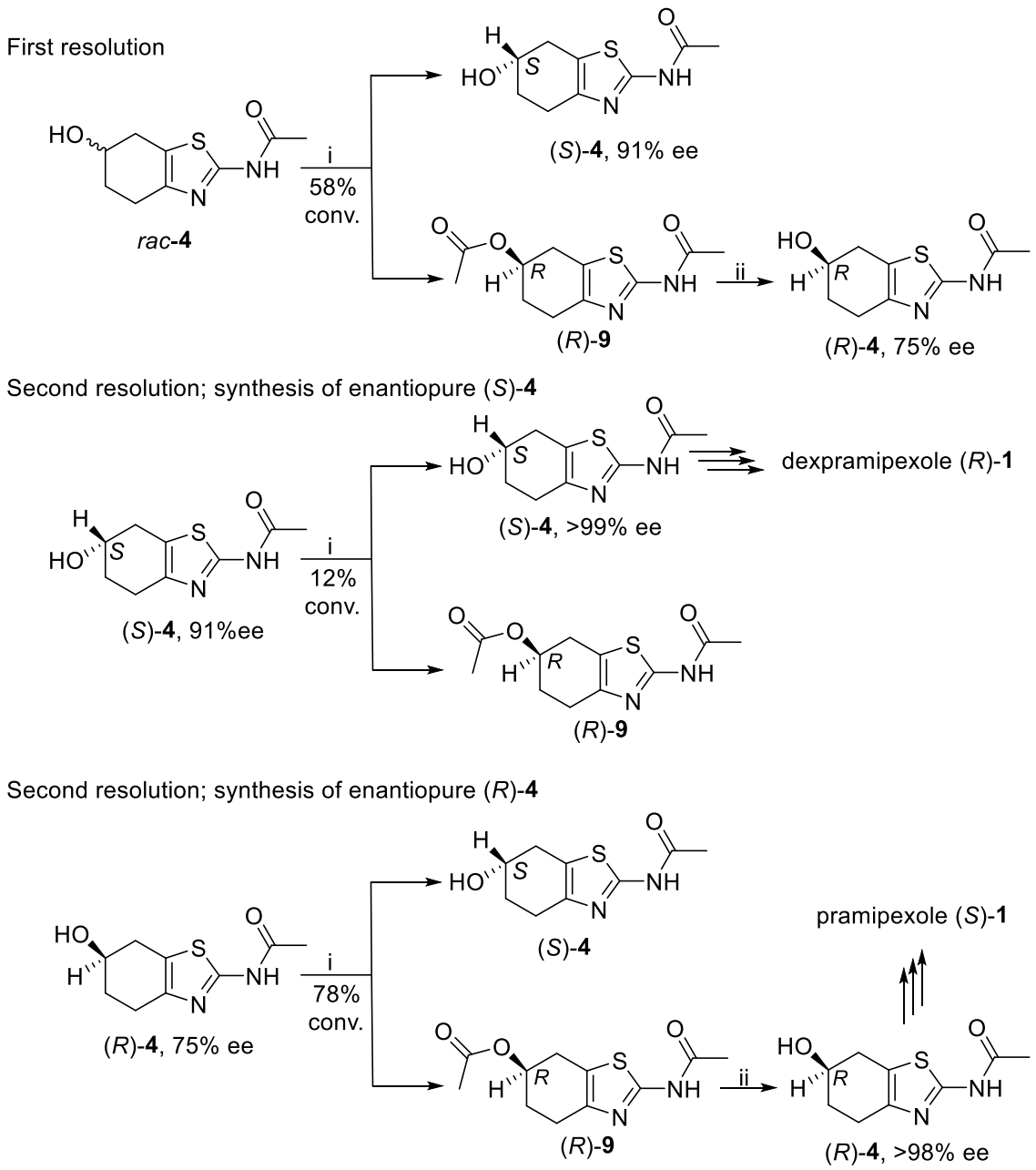

Scheme 6. CAL-A-catalyzed kinetic resolution of (*S*)- and (*R*)-**4**. (**i**) CAL-A, vinyl acetate, acetone; (**ii**) 1% NaOH, methanol.

2.2. X-ray Crystallography

The 3D structures of (*R*)-**4** and (*S*)-**4** were unambiguously determined by means of single-crystal X-ray diffraction and are reported in Figure 4 as ORTEP [32] representations. Both compounds crystallized in the monoclinic $P2_1$ space group: the asymmetric unit (ASU) of (*R*)-**4** shows the (*R*)-alcohol interacting with an ordered water molecule, while in (*S*)-**4** the ASU accommodates two independent molecules of the (*S*)-enantiomer.

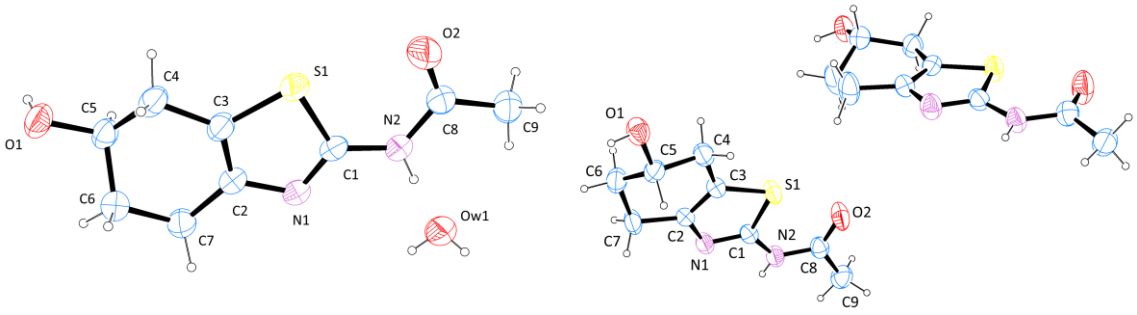

Figure 4. ORTEP [32] drawings of (*R*)-**4** (left) and (*S*)-**4** (right), with the arbitrary atom numbering (ellipsoids are at 40% probability and H atoms are represented as spheres of arbitrary radii). In (*S*)-**4**, the A-labeled molecule in the asymmetric unit (ASU) follows the scheme reported for the other molecule.

Overall, the two compounds are characterized by a flat region corresponding to the thiazole ring of the tetrahydrobenzothiazole, with the amide moiety lying on the same plane; the C9 methyl group deviates slightly, forming an angle of 6.1(1)° in (*R*)-**4**, and 8.1(1)° and 8.8(1)° in (*S*)-**4**. The cyclohexene moiety is in half-chair conformation, with the shared C2-C3 double bond belonging to the plane formed by the heterocycle. The Cremer–Pople [33] ring puckering parameters for the six-membered ring are Q_T = 0.4807(1)Å, θ = 128.9(1)° for (*R*)-**4**, and Q_T = 0.4870(1)[0.4737(1)Å], θ = 50.5(1)°[47.4(1)] for (*S*)-**4** (the values in the square brackets refer to the A-labeled molecule). The different θ values indicate that the cyclohexene ring assumes opposite half-chair conformations in the two enantiomers, while the two hydroxyl groups remain equatorially oriented in both structures. Moreover, the puckering data evidence small differences in the shape of the cyclohexenes in (*S*)-**4**, which justifies the presence of two distinct molecules in the crystal ASU. The superposition of the two forms of (*S*)-**4** is shown in Figure 5, which reveals that their most significant structural difference is represented by the torsion angles ε (*ε* = H1-O1-C5-C6) involving the hydroxyl group, which are 66.7(1)° and 27.1(1)°.

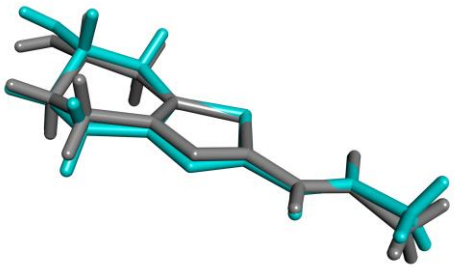

Figure 5. Superposition of the two independent molecules of the asymmetric unit of (*S*)-**4**.

The analysis of the intermolecular contacts shows considerable differences between the two crystals, even though hydrogen bonds remain the principal driving force in the solid-state assembly (Figure 6). In (*R*)-**4**, four H-bonds consolidate the crystal packing, with the water playing a central role in bridging the alcohol molecules: its oxygen interacts with the amidic hydrogen, while the two hydrogens form contacts involving the oxygens of the hydroxyl and amide functions. Overall, the water molecules create channels, crossing the crystal along the *c* axis (Figure 7). Another H-bond is established between the hydrogen of the hydroxyl group and the nitrogen of the thiazole ring. The crystal structure of (*S*)-**4** is stabilized by just two hydrogen bonds, between the amidic hydrogen and the hydroxyl oxygen, and between the alcoholic hydrogen and the C=O of the amide group. No intermolecular interactions are observed between the two independent molecules of the ASU. A summary of the H-bonds of (*R*)-**4** and (*S*)-**4** is reported in Table 5, along with a complete account of their geometry.

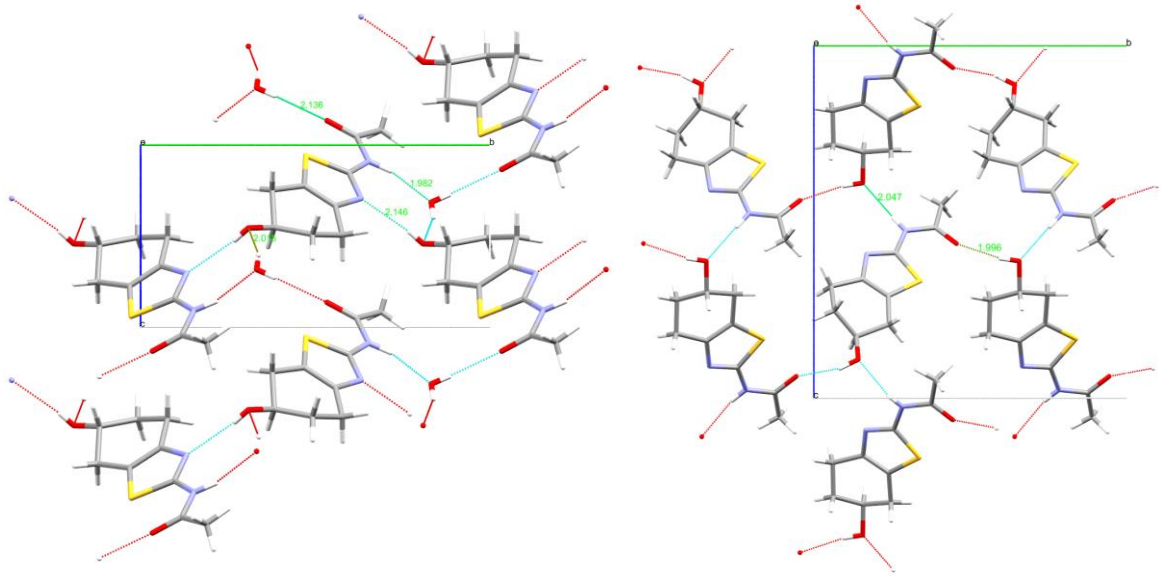

Figure 6. The dashed lines show the intermolecular contacts of (*R*)-**4** (left) and of (*S*)-**4** (right), viewed along the *a* axis.

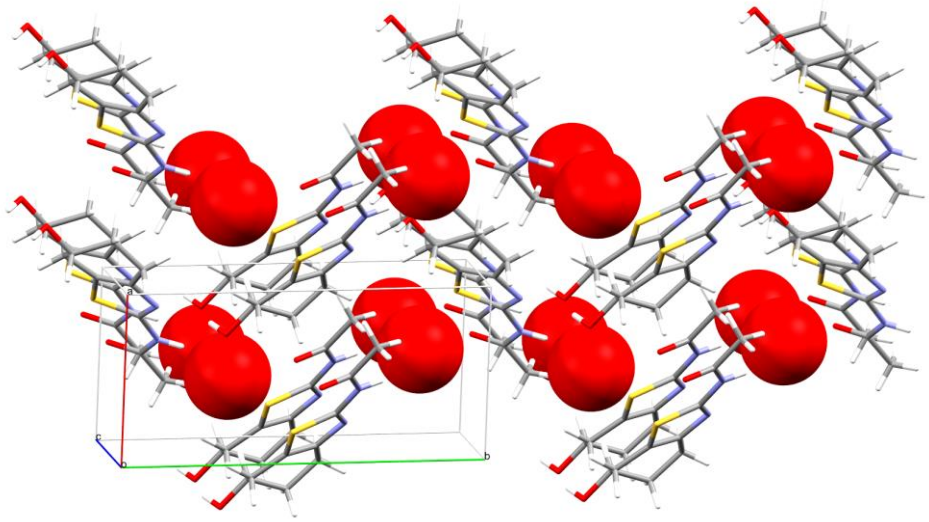

Figure 7. The spacefill representation of the water molecules in (*R*)-**4** evidences the presence of water channels in the crystal structure (shown along the *c* direction).

Table 5. Hydrogen-bond geometry of (*R*)-**4** and (*S*)-**4** (arbitrary atom-numbering scheme used in Figure 4). Values in square brackets refer to the A-labeled molecule in the ASU of (*S*)-**4**.

(*R*)-4				(*S*)-4			
H-Bond	**H···A (Å)**	**D···A (Å)**	**D-H···A (°)**	**H-Bond**	**H···A (Å)**	**D···A (Å)**	**D-H···A (°)**
N2-H2···Ow1	1.98(1)	2.815(1)	162.7(1)	O1-H1···O2A	1.94(1) [2.00(1)]	2.767(1) [2.814(1)]	162.8(1) [169.6(1)]
Ow1-H1A···O1	2.02(1)	2.760(1)	158.4(1)	N2-H2···O1A	2.05(1) [2.07(1)]	2.853(1) [2.828(1)]	174.8(1) [165.1(1)]
Ow1-H1B···O2	2.13(1)	2.826(1)	171.8(1)	-	-	-	-
O1-H1···N1	2.15(1)	2.815(1)	164.0(1)	-	-	-	-

3. Materials and Methods

3.1. Materials and Reagents

All employed solvents and reagents were purchased from Sigma-Aldrich (Merck Life Science S.r.l., Milano, Italy) and used without any further purification. Lipase B *Candida antarctica* (CAL-B, Novozym® 435, ≥10000 U/g), lipase A *Candida antarctica* (CAL-A, Immobead 150, 1620 U/g), lipase from *Candida rugosa* (CCL, 6.54 U/mg), lipase from *Pseudomonas fluorescens* (PFL, 40.2 U/mg), lipase from *Aspergillus niger* (194 U/mg), lipase from porcine pancreas (PPL, 23.9 U/mg) and lipase F-AP15 from *Rhizopus orizae* (165 U/mg) were purchased from Sigma-Aldrich (Merck Life Science S.r.l., Milano, Italy). The protease Alcalase CLEA (946 U/g) were purchased from CLEA Technologies (CLEA Technologies, Delft, The Netherlands).

3.2. Instrumentation

TLC analyses were performed on silica gel 60 F_{254} plates, precoated with a fluorescent indicator (Merck Life Science S.r.l., Milano, Italy), with detection by a 254 nm ultraviolet (UV) lamp. Column chromatography purifications were performed on silica gel 60 (70–230 mesh) (Merck Life Science S.r.l., Milano, Italy), 1:20 *w*/*w* substrate/silica gel.

The employed HPLC unit was a Merck-Hitachi (Hitachi Ltd., Tokyo, Japan), equipped with a UV detector model L-4250, pump system model L-6200 and a chromato-integrator model D-2500. The column employed in the analyses was a Daicel Chiralpak IA (Daicel Group, Chiral Technologies Europe, Illkirch Cedex, France). The dimension of the column is 250 mm × 4.6 mm, 5 µm. The elution was in isocratic mode with *n*-hexane/2-propanol 8:2. The flow rate was 0.7 mL/min. All the samples were measured at λ = 254 nm and 25 °C. Representative retention times (R_t): (*R*)-**4** 10.7 min; (*S*)-**4** 15.3 min; (*R*)- and (*S*)-**9** were not resolved and eluted at about 13.6 min. In order to establish the enantiomeric excess of acetate **9**, the compound was hydrolyzed with sodium hydroxide in methanol (1% *w*/*v*) to the corresponding alcohol **4**.

High-resolution mass spectra (HRMS) were recorded on Impact HDTM UHR-QqToF (Bruker Daltonics, Billerica, MA, USA); acquisition parameters were set as follows: Funnel1 RF 400 Vpp, Funnel2 RF 400 Vpp, Hexapole RF 600 Vpp, transfer time 95 µs, pre-pulse storage 12 µs, 40–650 *m*/*z* window. Calibration was performed online using ESI-L Low Concentration Tuning Mix (Agilent Technologies); the samples were dissolved in methanol at a final concentration of 0.1 µg/mL and injected at an infusion rate of 3 µL/min. Data acquisition and analysis were accomplished with Bruker Compass Data Analysis 4.1 software (Bruker Compass, Billerica, MA, USA).

Nuclear magnetic resonance (NMR) spectra were recorded on an AVANCE 500 spectrometer (Bruker, Billerica, MA, USA) equipped with a 5 mm broadband inverse probe (BBI) with field z-gradient operating at 500.13 and 125.76 MHz for ^{1}H and ^{13}C, respectively. NMR spectra were recorded at 300 K in $CDCl_3$ (isotopic enrichment 99.95%) solution. The data were collected and processed by XWIN-NMR software (3.5, Bruker) running on a PC with Microsoft Windows 7 (Redmond, WA, USA). The samples (10 mg), were dissolved in $CDCl_3$ (0.75 mL) in a 5 mm NMR tube. Acquisition parameters for 1D were as follows: ^{1}H spectral width of 5000 Hz and 32 K data points providing a digital resolution of ca. 0.305 Hz per point, relaxation delay 10 s; ^{13}C spectral width of 29,412 Hz and 64 K data points providing a digital resolution of ca. 0.898 Hz per point, relaxation delay 2 s. The experimental error in the measured ^{1}H-^{1}H coupling constants was ± 0.5 Hz. Chemical shifts (δ) of the ^{1}H NMR and ^{13}C NMR spectra are reported in ppm using the signal for residual solvent resonance as internal standard (^{1}H NMR: $CDCl_3$ 7.26 ppm; ^{13}C NMR: $CDCl_3$ 77.0 ppm (central line)). The splitting pattern abbreviations are as follows: s, singlet; d, doublet; t, triplet; q, quartet; m, multiplet, and bs, broad signal. For two-dimensional experiments, Bruker microprograms using gradient selection (gs) were applied. All two-dimensional spectra (COSY and HSQC) were acquired with 2048 data points for t_2 and 256 for t_1 increments. The confirmation of the structure of compounds **9** was obtained by NMR analysis, in particular through proton and carbon 1D-NMR spectra, as well as by 2D-NMR homo-correlation (COSY) and hetero-correlation (HSQC) experiments.

The NMR and HRMS spectra, and the HPLC chromatograms are available in the supplementary materials.

3.3. Chemistry

Compounds **4** and **8** were synthesized according to the methods previously described in Ref. [15].

3.3.1. *rac*-2-Acetamido-4,5,6,7-tetrahydrobenzo[d]thiazol-6-yl Acetate (*rac*-**9**)

To a solution of *rac*-**4** (1.0 g, 4.7 mmol) in anhydrous pyridine (12 mL) acetic anhydride (0.9 mL, 9.5 mmol) was added. The reaction mixture was stirred at room temperature overnight. The reaction progress was monitored by TLC analysis (dichloromethane/methanol 95:5). After complete conversion, the reaction mixture was diluted with water (60 mL) and extracted with dichloromethane (3 x 30 mL). The combined organic phases were dried over sodium sulfate and, after filtration, evaporated at reduced pressure affording *rac*-**9** as a white solid (1.1 g, 4.3 mmol, 91%).
Rf 0.6. ^{1}H NMR ($CDCl_3$, δ, ppm): 5.26 (m, 1H, H-6), 3.06 (dd, J = 16.3 e 4.8 Hz, 1H, H_a-7), 2.85–2.68 (m, 3H, H_b-7, H_a-4 e H_b-4), 2.23 (s, 3H, $NHCOCH_3$), 2.13–1.98 (m, 2H, H_a-5 e H_b-5), 2.05 (s, 3H, $OCOCH_3$). ^{13}C NMR (CDCl3, δ, ppm): 170.6 ($OCOCH_3$), 167.6 ($NHCOCH_3$), 157.2 (C-2), 142.1 (C-N), 119.6 (C-S), 68.7 (C-6), 28.5 (C-7), 27.4 (C-5), 23.2 ($NHCOCH_3$), 23.0 (C-4), 21.2 ($OCOCH_3$). HRMS (ESI) m/z: Calcd. for $C_{11}H_{15}N_2O_3S$ $[M + H]^+$ 255.0803. Found 255.0796.

3.3.2. General Procedure for Enzyme-Catalyzed Hydrolysis

rac-2-Acetamido-4,5,6,7-tetrahydrobenzo[d]thiazol-6-yl acetate (*rac*-**9**) (13 mg; 0.05 mmol) was suspended in phosphate buffer pH 7 (5 mL) in a 10 mL glass vial followed by addition of the enzyme (an amount corresponding to about 100 U). The mixture was shaken at 300 rpm and room temperature. A sample of about 50 µL was collected regularly, diluted with water, and extracted with ethyl acetate. The organic phase was concentrated under reduced pressure. The residue was dissolved in 2-propanol (about 50 µL) and a portion (10 µL) was injected in a HPLC system equipped with a Chiralpak IA column.

3.3.3. General Procedure for Enzyme-Catalyzed Transesterification

rac-N-(6-Hydroxy-4,5,6,7-tetrahydrobenzo[d]thiazol-2-yl)acetamide (*rac*-**4**) (10 mg; 0.05 mmol) was dissolved or suspended in the organic solvent (5 mL) in a 10 mL glass vial followed by addition of vinyl acetate (14 µL; 0.15 mmol) and the enzyme (an amount corresponding to about 100 U). The mixture was shaken at 300 rpm and room temperature. A sample of about 50 µL was collected regularly and concentrated under reduced pressure. The residue was dissolved in 2-propanol (about 50 µL) and a portion (10 µL) was injected in a HPLC system equipped with a Chiralpak IA column.

3.3.4. Lipase-Catalyzed Synthesis of Enantioenriched (*S*)-N-(6-Hydroxy-4,5,6,7-tetrahydrobenzo[d]thiazol-2-yl)acetamide [(*S*)-**4**]

To a solution of *rac*-**4** (500 mg, 2.4 mmol) in anhydrous acetone (200 mL) and *n*-hexane (50 mL), vinyl acetate (0.7 mL, 7.6 mmol) and CAL-A (3 g, 4860 U) were added sequentially. The reaction mixture was shaken at room temperature and 300 rpm in a screw-cap flask. The reaction progress was monitored by HPLC, equipped with a Chiralpak IA column. At 58% conversion (reaction time: about 300 h), the enzyme was removed by filtration and the solvent was evaporated at reduced pressure. The residue was purified by silica gel column chromatography. By elution with *n*-hexane/ethyl acetate 6:4, acetate (*R*)-**9** was recovered (328 mg, 54%). Elution with dichloromethane/methanol 95:5 afforded enantioenriched (*S*)-**4** (190 mg, 38%, 91% ee).

3.3.5. Hydrolysis of Enantioenriched (*R*)-2-Acetamido-4,5,6,7-tetrahydrobenzo[d]thiazol-6-yl Acetate [(*R*)-**9**] to Enantioenriched (*R*)-**4**

A solution of 1% *w*/*v* sodium hydroxide in methanol (15 mL, 3.8 mmol) and enantioenriched (*R*)-**9** (300 mg, 1.18 mmol), obtained from the enzyme-catalyzed resolution described in Section 3.3.4, was stirred at room temperature. The reaction progress was monitored by TLC analysis (dichloromethane/methanol 95:5) until starting material disappearance (2 h). The pH of the reaction mixture was adjusted to 7 by addition of 1 M HCl and methanol was removed under reduced pressure. Water was added (5 mL) and the obtained aqueous phase was extracted with ethyl acetate (5 × 5 mL). The collected organic phases were dried over sodium sulfate; after filtration, the solvent was removed at reduced pressure, affording enantioenriched (*R*)-**4** (212 mg, 1.0 mmol, 85%) which was used directly in the next step without any further purification. The 75% ee of enantioenriched (*R*)-**4** was determined by HPLC analysis on a Chiralpak IA column.

3.3.6. Lipase-Catalyzed Synthesis of Enantiopure (*S*)-N-(6-Hydroxy-4,5,6,7-tetrahydrobenzo[d]thiazol-2-yl)acetamide [(*S*)-**4**]

To a solution of enantioenriched (*S*)-**4** (150 mg, 0.71 mmol, 91% ee), obtained as described in Section 3.3.4, in anhydrous acetone (60 mL) and *n*-hexane (15 mL), vinyl acetate (210 µL, 2.3 mmol) and CAL-A (0.9 g, 1458 U) were sequentially added. The reaction mixture was shaken at room temperature and 300 rpm in a screw-cap flask. The reaction progress was monitored by HPLC equipped with a Chiralpak IA column. The reaction was stopped at 12% conversion (reaction time: about 48 h), the enzyme was removed by filtration and the solvent was evaporated at reduced pressure. The residue was purified by silica gel column chromatography. By elution with *n*-hexane/ethyl acetate 6:4, acetate (*R*)-**9** was recovered (18 mg, 10%). Elution with dichloromethane/methanol 95:5 afforded enantiopure (*S*)-**4** (123 mg, 82%, >99% ee). The chemical-physical properties of (*S*)-**4** were in agreement with the reported ones [15].

3.3.7. Lipase-Catalyzed Synthesis of Enantiopure (*R*)-2-Acetamido-4,5,6,7-tetrahydrobenzo[d]thiazol-6-yl Acetate [(*R*)-**9**]

To a solution of enantioenriched (*R*)-**4** (200 mg, 0.94 mmol, 75% ee), obtained as described in Section 3.3.5, in anhydrous acetone (80 mL) and n-hexane (20 mL), vinyl acetate (280 µL, 3.02 mmol) and CAL-A (1.2 g, 1944 U) were added sequentially. The reaction mixture was shaken at room temperature and 300 rpm in a screw-cap flask. The reaction progress was monitored by HPLC equipped with a Chiralpak IA column. The reaction was stopped at 78% conversion (reaction time: about 144 h), the enzyme was removed by filtration and the solvent was evaporated at reduced pressure. The residue was purified by silica gel column chromatography. By elution with *n*-hexane/ethyl acetate 6:4, acetate (*R*)-**9** was recovered (174 mg, 72%,). Elution with dichloromethane/methanol 95:5 afforded (*S*)-**4** (30 mg, 15%).

3.3.8. Hydrolysis of Enantiopure (*R*)-2-Acetamido-4,5,6,7-tetrahydrobenzo[d]thiazol-6-yl Acetate [(*R*)-**9**] to Enantiopure (*R*)-**4**

The hydrolysis of enantiopure (*R*)-**9** (100 mg, 0.39 mmol), obtained from the enzyme-catalyzed resolution described in Section 3.3.7, was carried out under the same conditions described in Section 3.3.5 affording enantiopure (*R*)-**4** (74 mg, 0.35 mmol, 90%). The >98% ee of enantiopure (*R*)-**4** was determined by HPLC analysis on a Chiralpak IA column. The chemical-physical properties of (*R*)-**4** were in agreement with the reported ones [15].

3.4. X-ray Crystallography

Diffraction-quality crystals were obtained at room temperature by slow evaporation of an ethanol/water 1:1 solution for (*R*)-**4**, and of a methanol/water 1:1 solution for (*S*)-**4**. After a week, transparent crystals precipitated as prisms.

X-ray diffraction data for (*R*)-**4** were collected at room temperature on a Bruker Apex II CCD diffractometer, using graphite-monochromatized Mo-Ka X-radiation (λ = 0.71073 Å); for (*S*)-**4**, a Bruker-Axs CCD-based three-circle diffractometer was used, working with the same X-ray source (λ = 0.7107 Å) and environmental conditions.

The collected information was processed with the SAINT [34] software for data reduction (including intensity integration, background, Lorentz and polarization corrections) and for the determination of accurate unit-cell dimensions. Absorption effects were empirically evaluated by the SADABS [35] software, and absorption correction was applied to the data. The structures were solved by direct methods (SIR-14) [36] and completed by iterative cycles of full-matrix least squares refinement on Fo^2 and DF synthesis using SHELXL-17 [37] on the WingX.v2014.1 suite [38]. The hydrogen atoms bonded to carbons were included at geometrically calculated positions and refined using a riding model. CCDC entries 1994275 [(R)-**4**] and 1994277 [(S)-**4**] contain the supplementary crystallographic data for this paper.

Crystal data for (*R*)-**4**: $C_9H_{12}N_2O_2S{\cdot}H_2O$, M_r = 230.28 g/mol, Monoclinic, Space group $P2_1$, a = 6.5701(4) Å, b = 12.6906(7) Å, c = 6.9136(4) Å, β = 107.12(1), V = 550.90(5) Å^3, Z = 2, D_{calc} = 1.388 Mg/m^3, F(000) = 244, R = 0.040 for 3074 reflections with $Fo > 4sig(Fo)$ (R = 0.048 for all 3416 unique/6449 collected reflections), $wR2$ = 0.093 for reflections with $Fo > 4sig(Fo)$ ($wR2$ = 0.098 for all unique reflections), T = 293(2) K, GOF = 1.156. The reflections were collected in the range 3.08° ≤ θ ≤ 31.64° (limiting indices = -9 ≤ h ≤ 9, -17 ≤ k ≤ 18, -9 ≤ l ≤ 9) employing a 0.36 × 0.20 × 0.05 mm crystal. The residual positive and negative electron densities in the final map were 0.357 and -0.186 Å^{-3}.

Crystal data for (*S*)-**4**: $C_9H_{12}N_2O_2S$, M_r = 424.53 g/mol (212.27 g/mol for each molecule), monoclinic, space group $P2_1$, a = 5.0452(3) Å, b = 13.3800(8) Å, c = 15.0609(3) Å, β = 90.04(1), V = 1016.7(1) Å^3, Z = 2, D_{calc} = 1.387 Mg/m^3, F(000) = 448, R = 0.051 for 2737 reflections with $Fo > 4sig(Fo)$ (R = 0.059 for all 3172 unique/7389 collected reflections), $wR2$ = 0.123 for reflections with $Fo > 4sig(Fo)$ ($wR2$ = 0.128 for all unique reflections), T = 293(2) K, GOF = 1.005. The reflections were collected in the range 1.35° ≤ θ ≤ 24.01° (limiting indices = -5 ≤ h ≤ 5, -15 ≤ k ≤ 15, -17 ≤ l ≤ 17) employing a 0.25 × 0.16 × 0.03 mm crystal. The residual positive and negative electron densities in the final map were 0.357 and −0.243 Å^{-3}.

4. Conclusions

The bicyclic compound pramipexole is a pharmacologically active substance, showing anti-Parkinson effects only when its stereocenter has the (*S*)- configuration. Conversely, its (*R*)-enantiomer is still under investigation to identify possible therapeutic applications. For these reasons, we planned to prepare the optically pure synthons of (*R*)- and (*S*)-pramipexole, by means of the enzymatic resolution of the suitable secondary alcohol. This result was achieved through a double kinetic resolution, catalyzed by CAL-A; the reaction conditions were studied and optimized, also considering the choice of the solvent. Starting from the racemic alcohol **4**, a 4:1 *v*/*v* mixture of acetone/*n*-hexane allowed us to obtain the (*R*)-alcohol **4** and (*S*)-alcohol **4** in >98% ee and >99% ee and 30% and 31% overall yields, respectively. The single-crystal X-ray analysis of these compounds unambiguously defined the 3D structural features of the two enantiomers and revealed a considerably different crystal packing.

These two advanced chiral intermediates can be converted to (*S*)- and (*R*)-pramipexole following the synthetic route previously optimized in our laboratory. A comparison between the two biocatalytic approaches put in evidence that the previous method, consisting in the enantioselective reduction of the suitable ketone **3** catalyzed by *Saccharomyces cerevisiae*, provided only the (*R*)-alcohol **4** in >98% ee. The (*S*)- alcohol **4** was obtained, starting from the (*R*)- alcohol **4**, through an inversion of configuration operated by means of the Mitsunobu reaction that furnished a complex crude reaction mixture. After a careful purification process the (*S*)- alcohol **4** was recovered in poor yield (27%). By contrast, the new chemoenzymatic approach afforded both the (*R*)- and (*S*)-alcohol **4** in good yields (30% and 31% overall yields, respectively) starting from *rac*-**4**; this is a remarkable result considering that, with an enzymatic kinetic resolution of a racemate, the maximum theoretical yield for each enantiomer is 50%.

Supplementary Materials: The following are available online at www.mdpi.com/2073-4344/10/8/941/s1, Figure S1: 1H NMR of compound **9**, Figure S2: ^{13}C NMR of compound **9**, Figure S3: COSY of compound **9**, Figure S4: HSQC of compound **9**, Figure S5: HRMS of compound **9**, Figure S6: MS-MS of compound **9**, Figure S7: Lipase-catalyzed synthesis of enantioenriched (*S*)-*N*-(6-hydroxy-4,5,6,7-tetrahydrobenzo[d]thiazol-2-yl)acetamide [(*S*)-**4**]. HPLC analysis of the crude reaction mixture, Figure S8: Lipase-catalyzed synthesis of enantioenriched (*S*)-*N*-(6-hydroxy-4,5,6,7-tetrahydrobenzo[d]thiazol-2-yl)acetamide [(*S*)-**4**]. HPLC analysis of the purified (*S*)-**4**, Figure S9: Lipase-catalyzed synthesis of enantioenriched (*S*)-*N*-(6-hydroxy-4,5,6,7-tetrahydrobenzo[d]thiazol-2-yl)acetamide [(*S*)-**4**]. HPLC analysis of the purified and hydrolyzed (*R*)-**9**, Figure S10: Lipase-catalyzed synthesis of enantiopure (*S*)-*N*-(6-hydroxy-4,5,6,7-tetrahydrobenzo[d]thiazol-2-yl)acetamide [(*S*)-**4**]. HPLC analysis of the crude reaction mixture, Figure S11: Lipase-catalyzed synthesis of enantiopure (*S*)-*N*-(6-hydroxy-4,5,6,7-tetrahydrobenzo[d]thiazol-2-yl)acetamide [(*S*)-**4**]. HPLC analysis of the purified (*S*)-**4**, Figure S12: Lipase-catalyzed synthesis of enantiopure (*R*)-2-Acetamido-4,5,6,7-tetrahydrobenzo[d]thiazol-6-yl acetate [(*R*)-**9**]. HPLC analysis of the crude reaction mixture, Figure S13: Lipase-catalyzed synthesis of enantiopure (*R*)-2-Acetamido-4,5,6,7-tetrahydrobenzo[d]thiazol-6-yl acetate [(*R*)-**9**]. HPLC analysis of the purified and hydrolyzed (*R*)-**9**.

Author Contributions: Conceptualization of the work: P.F. and P.G.; synthesis: S.C. and S.R.E.; crystallographic analysis: F.M., C.C. and M.M.; HPLC and NMR analysis: S.C.; writing—original draft preparation, review and editing: F.M., P.F., M.M. and S.C.; supervision: P.F. All authors have read and agreed to the published version of the manuscript.

Funding: This research received no external funding.

Acknowledgments: S.C. thanks Farmhispania S.A. (Barcelona, Spain) for a research fellowship. We thank Fulvio Magni and Clizia Chinello (Department of Medicine and Surgery, University of Milano-Bicocca, Clinical Proteomics and Metabolomics Unit, Vedano al Lambro, Italy) for HRMS spectra.

Conflicts of Interest: The authors declare no conflict of interest.

References

1. Antonini, A.; Barone, P.; Ceravolo, R.; Fabbrini, G.; Tinazzi, M.; Abbruzzese, G. Role of Pramipexole in the Management of Parkinson's Disease. *Cns. Drugs* **2010**, *24*, 829–841.
2. Hametner, E.M.; Seppi, K.; Poewe, W. Role and clinical utility of pramipexole extended release in the treatment of early Parkinson's disease. *Clin. Interv. Aging* **2012**, *7*, 83–88.
3. Lloret, S.P.; Rascol, O. Pramipexole extended-release (once-daily formulation) for the treatment of Parkinson's disease. *Expert Opin. Pharmaco.* **2010**, *11*, 2221–2230.
4. Bozik, M.E.; Mather, J.L.; Kramer, W.G.; Gribkoff, V.K.; Ingersoll, E.W. Safety, tolerability, and pharmacokinetics of KNS-760704 (dexpramipexole) in healthy adult subjects. *J. Clin. Pharmacol* **2011**, *51*, 1177–1185.
5. Gribkoff, V.K.; Bozik, M.E. KNS-760704 [(6R)-4,5,6,7-tetrahydro-N6-propyl-2, 6-benzothiazole-diamine dihydrochloride monohydrate] for the treatment of amyotrophic lateral sclerosis. *Cns. Neurosci. Ther.* **2008**, *14*, 215–226.
6. Wang, H.; Larriviere, K.S.; Keller, K.E.; Ware, K.A.; Burns, T.M.; Conaway, M.A.; Lacomis, D.; Pattee, G.L.; Phillips, L.H.; Solenski, N.J., et al. R(+) pramipexole as a mitochondrially focused neuroprotectant: Initial early phase studies in ALS. *Amyotroph. Lateral Sc.* **2008**, *9*, 50–58.
7. Cudkowicz, M.; Bozik, M.E.; Ingersoll, E.W.; Miller, R.; Mitsumoto, H.; Shefner, J.; Moore, D.H.; Schoenfeld, D.; Mather, J.L.; Archibald, D., et al. The effects of dexpramipexole (KNS-760704) in individuals with amyotrophic lateral sclerosis. *Nat. Med.* **2011**, *17*, 1652-U1169.
8. Cudkowicz, M.E.; van den Berg, L.H.; Shefner, J.M.; Mitsumoto, H.; Mora, J.S.; Ludolph, A.; Hardiman, O.; Bozik, M.E.; Ingersoll, E.W.; Archibald, D., et al. Dexpramipexole versus placebo for patients with amyotrophic lateral sclerosis (EMPOWER): a randomised, double-blind, phase 3 trial. *Lancet. Neurol.* **2013**, *12*, 1059–1067.
9. Dworetzky, S.I.; Hebrank, G.T.; Archibald, D.G.; Reynolds, I.J.; Farwell, W.; Bozik, M.E. The targeted eosinophil-lowering effects of dexpramipexole in clinical studies. *Blood Cell Mol. Dis.* **2017**, *63*, 62–65.
10. Panch, S.R.; Bozik, M.E.; Brown, T. Dexpramipexole as an oral steroid-sparing agent in hypereosinophilic syndromes (vol 132, pg 501, 2018). *Blood* **2018**, *132*, 1461–1461.

11. Pospisilik, K. Process for resolution of 2-amino-6-propylamino-4,5,6,7-tetrahydrobenzothiazole. WO2002022591A1, 2002.
12. Schneider, C.S.; Mierau, J. Dopamine Autoreceptor Agonists - Resolution and Pharmacological Activity of 2,6-Diaminotetrahydrobenzothiazole and an Aminothiazole Analog of Apomorphine. *J. Med. Chem* **1987**, *30*, 494–498.
13. Keil, A.; Schulte, M. Process for the purification of pramipexole using chiral chromatography. WO2006003471A2, 2006.
14. Pathare, D.B.; Jadhav, A.S.; Shingare, M.S. Validated chiral liquid chromatographic method for the enantiomeric separation of pramipexole dihydrochloride monohydrate. *J. Pharmaceut Biomed.* **2006**, *41*, 1152–1156.
15. Ferraboschi, P.; Ciceri, S.; Ciuffreda, P.; De Mieri, M.; Romano, D.; Grisenti, P. Baker's yeast catalyzed preparation of a new enantiomerically pure synthon of (S)-pramipexole and its enantiomer (dexpramipexole). *Tetrahedron-Asymmetr.* **2014**, *25*, 1239–1245.
16. Riva, S.; Fassi, P.; Scarpellini, M.; Allegrini, P.; Razzetti, G. Lipase catalyzed kinetic resolution of ethyl 2-(acetylamino)-4,5,6,7-tetrahydro-6-benzothiazolecarboxyate. EP1808492A1, 2007.
17. Valivety, R.H.; Michels, P.C.; Pantaleone, D.P.; Khmelnitsky, Y.L. Biocatalytic process for preparing enantiomerically enriched pramipexole. WO2006012277A2, 2006.
18. Ferraboschi, P.; Chiara Sala, M.; Stradi, R.; Ragonesi, L.; Gagliardi, C.; Lanzarotti, P.; Ragg, E.M.; Mori, M.; Meneghetti, F. Full spectroscopic characterization of two crystal pseudopolymorphic forms of the antiandrogen cortexolone 17alpha-propionate for topic application. *Steroids* **2017**, *128*, 95–104.
19. Meneghetti, F.; Ferraboschi, P.; Grisenti, P.; Reza Elahi, S.; Mori, M.; Ciceri, S. Crystallographic and NMR Investigation of Ergometrine and Methylergometrine, Two Alkaloids from Claviceps purpurea. *Molecules* **2020**, *25*.
20. Castaldi, G.; Bologna, A.; Allegrini, P.; Razzetti, G.; Lucchini, V. Method for preparing intermediates of pramipexole. WO2005092871A2, 2005.
21. Gotor-Fernandez, V.; Brieva, R.; Gotor, V. Lipases: Useful biocatalysts for the preparation of pharmaceuticals. *J. Mol. Catal. B-Enzym.* **2006**, *40*, 111–120.
22. Patel, R.N. Biocatalysis for synthesis of pharmaceuticals. *Bioorgan Med. Chem* **2018**, *26*, 1252–1274.
23. Sheldon, R.A.; Brady, D. The limits to biocatalysis: pushing the envelope. *Chem Commun* **2018**, *54*, 6088–6104.
24. Degueilcastaing, M.; Dejeso, B.; Drouillard, S.; Maillard, B. Enzymatic-Reactions in Organic-Synthesis .2. Ester Interchange of Vinyl Esters. *Tetrahedron. Lett.* **1987**, *28*, 953–954.
25. Wang, Y.F.; Lalonde, J.J.; Momongan, M.; Bergbreiter, D.E.; Wong, C.H. Lipase-Catalyzed Irreversible Transesterifications Using Enol Esters as Acylating Reagents - Preparative Enantioselective and Regioselective Syntheses of Alcohols, Glycerol Derivatives, Sugars, and Organometallics. *J. Am. Chem. Soc.* **1988**, *110*, 7200–7205.
26. Herbst, D.; Peper, S.; Niemeyer, B. Enzyme catalysis in organic solvents: influence of water content, solvent composition and temperature on Candida rugosa lipase catalyzed transesterification. *J. Biotechnol.* **2012**, *162*, 398–403.
27. Rakels, J.L.; Straathof, A.J.; Heijnen, J.J. A simple method to determine the enantiomeric ratio in enantioselective biocatalysis. *Enzyme Microb. Technol.* **1993**, *15*, 1051–1056.
28. Brown, S.M.; Davies, S.G.; de Sousa, J.A.A. Kinetic resolution strategies. II. Enhanced enantiomeric excesses and yields for the faster reacting enantiomer in lipase mediated kinetic resolutions. *Tetrahedron: Asymmetry* **1993**, *4*, 813.
29. Chen, C.S.; Fujimoto, Y.; Girdaukas, G.; Sih, C.J. Quantitative-Analyses of Biochemical Kinetic Resolutions of Enantiomers. *J. Am. Chem. Soc.* **1982**, *104*, 7294–7299.
30. Faber, K.; Kroutil, W. A Computer Program for the Determination of the Enantioselectivity (E-Value) in the Kinetic Resolution of Enantiomers. Availabe online: http://biocatalysis.uni-graz.at/enantio/DataFiles/Selectivity-Help.pdf (accessed on 13/01/2020).
31. Sih, C.J.; Wu, S.H. Resolution of Enantiomers Via Biocatalysis. *Top. Stereochem.* **1989**, *19*, 63–125.
32. Farrugia, L. ORTEP-3 for Windows - a version of ORTEP-III with a Graphical User Interface (GUI). *J. Appl. Crystallogr.* **1997**, *30*, 565.
33. Cremer, D.; Pople, J.A. General definition of ring puckering coordinates. *J. Am. Chem. Soc.* **1975**, *97*, 1354.
34. *Bruker: SAINT Software Reference Manual. Version 6, Bruker AXS Inc., Madison, Wisconsin, USA, 2003*.

35. Krause, L.; Herbst-Irmer, R.; Sheldrick, G.M.; Stalke, D. Comparison of silver and molybdenum microfocus X-ray sources for single-crystal structure determination. *J. Appl. crystallogr.* **2015**, *48*, 3–10.
36. Burla, M.C.; Caliandro, R.; Carrozzini, B.; Cascarano, G.L.; Cuocci, C.; Giacovazzo, C.; Mallamo, M.; Mazzone, A.; Polidori, G. Crystal structure determination and refinement via SIR2014. *J. Appl. Crystallogr.* **2015**, *48*, 306–309.
37. Sheldrick, G. Crystal structure refinement with SHELXL. *Acta Crystallogr., Section. C* **2015**, *71*, 3–8.
38. Farrugia, L. WinGX and ORTEP for Windows: an update. *J. Appl. Crystallogr.* **2012**, *45*, 849–854.